

# High Light Response Uniformity in Industrial Growth of 600-mm-Long BGO Crystals for Dark Matter Particle Explorer

Lanying Yuan<sup>1</sup>, Member, IEEE, Haihong Ni, Zhiming Ji, Junfeng Chen, Member, IEEE, Guilan Song, Xuejun Qi, Xiang Li, Shiyun Sun, and Shaohua Wang, Member, IEEE

**Abstract**—Hundreds of high-quality 25 mm × 25 mm × 600 mm Bi<sub>4</sub>Ge<sub>3</sub>O<sub>12</sub> single crystals were industrially grown by the Bridgman method for the Dark Matter Particle Explorer (DAMPE) project. With respect to the crystals with the best optical quality, the optical transmittance along the longitudinal and transversal directions can achieve 72% and 76% at 480 nm, respectively. Most of the grown crystals satisfied the light output uniformity requirement of the DAMPE calorimeter. For the remaining crystals, the effects of air annealing, reflector materials, and surface treatment on the improvement of light response uniformity were also studied.

**Index Terms**—Air annealing, light response uniformity (LRU), reflector materials, scintillator, surface treatment.

## I. INTRODUCTION

SCINTILLATORS can efficiently convert high-energy particles and radiation into light with a wavelength in or around the visible spectral regions, and they are widely used in nuclear medical imaging, oil logging, and high-energy physics applications. For the high-energy physics applications, in recent years, inorganic scintillating crystals were applied in the discovery of Higgs boson [1]. The use of a large number of lead tungstate (PbWO<sub>4</sub>) crystals as the key detection elements in the electromagnetic calorimeter of CMS experiment at CERN proves the critical status of inorganic scintillators for high-energy physics applications.

The search for dark matter in the universe is an important and challenging task. Physicists are devoted to designing experiments to find the evidences of the existence of dark matter, but few results were reported [2]. In 2015, China launched the Dark Matter Particle Explorer (DAMPE), the first space dark matter detection satellite, to find evidence for the existence of dark matter particles. It has been in operation for more than 2 years, and has acquired the most accurate high-energy cosmic ray energy spectra so far [3]. The Bi<sub>4</sub>Ge<sub>3</sub>O<sub>12</sub> (BGO) scintillating crystals as the direct medium for the possible

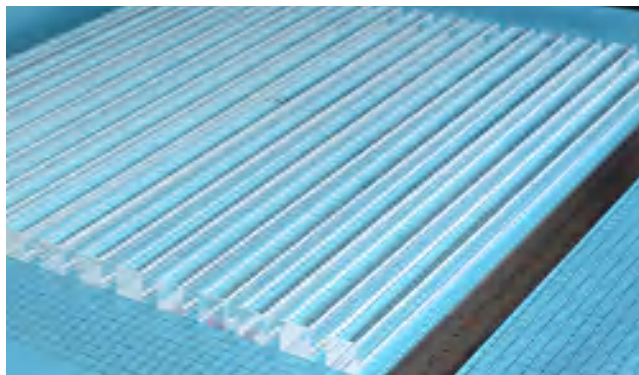


Fig. 1. Mass-produced 25 mm × 25 mm × 600 mm BGO single crystals.

annihilation of dark matter (energetic electrons and gamma rays) play an important role in the dark matter detection. The project required hundreds of 600-mm-long BGO crystals with high optical quality and light response uniformity (LRU). The LRU means the difference in the collection of scintillation light excited by gamma ray in different locations along the long axis of the crystal. Our previous work has reported the characterization of optical transmittance and energy resolution of the crystal SIC-BGO-125 [4], and also the linear correlation between optical transmittance and LRU of the 600-mm-long BGO crystals [5]. In this paper, we conducted a systematic study on statistical distribution of the LRN of industrial growth 600-mm-long BGO crystals, and carried out posttreatment process studies to optimize the initial unsatisfied crystal, such as air annealing, reflector materials, and crystal surface treatment with the dual-end readout mode and the specified PMTs according to the application and design of DAMPE.

## II. INDUSTRIAL PRODUCED BGO CRYSTALS

All the 600-mm-long BGO crystals were grown by the Bridgman method at the Shanghai Institute of Ceramics, Chinese Academy of Sciences. The typical mass-produced BGO crystals with the dimensions of 25 mm × 25 mm × 600 mm are shown in Fig. 1. The as-grown crystals are colorless, crack free, and visible inclusion free.

## III. MEASUREMENT METHODS

The optical transmission spectra of the BGO crystals and the reflectivity of the reflector materials were measured by a

Manuscript received March 12, 2018; revised May 14, 2018; accepted May 31, 2018. Date of publication June 8, 2018; date of current version July 16, 2018. This work was supported by the National Science Foundation of China under Grant 51602323. (Corresponding author: Lanying Yuan.)

The authors are with the Shanghai Institute of Ceramics, Chinese Academy of Sciences, Shanghai 201899, China (e-mail: lyuan@mail.sic.ac.cn).

Color versions of one or more of the figures in this paper are available online at <http://ieeexplore.ieee.org>.

Digital Object Identifier 10.1109/TNS.2018.2844459

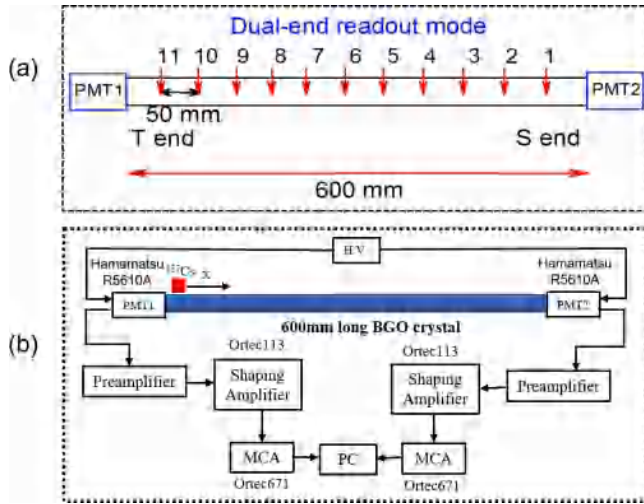


Fig. 2. Schematic of (a) test principle of the LRU and (b) pulse processing chain for the LO acquisition.

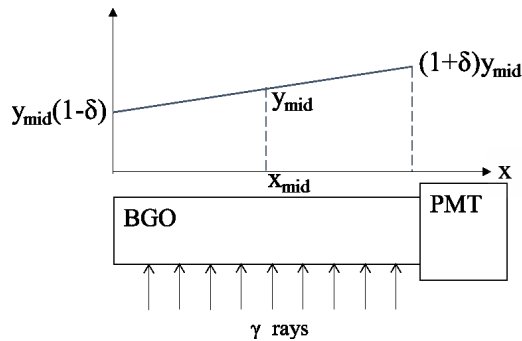


Fig. 3. Schematic of the LRU.

Perkin Elmer Lambda 950 spectrophotometer equipped with a general purpose optical bench with a spectralon-coated integrating sphere and beam apertures. The systematic uncertainty in repeated measurements was determined to be 0.2%.

The light output (LO) of BGO crystal was measured using Hamamatsu R5610A PMTs with a borosilicate glass window and by irradiating the crystal with a collimated  $^{137}\text{Cs}$   $\gamma$ -rays source (2  $\mu\text{Ci}$ ) at 11 positions evenly distributed along the crystal's longitudinal axis (means the direction of the longer optical path [Fig. 2(a)]. All other faces of the samples were wrapped with the reflector materials. The schematic of the pulse processing chain is presented in Fig. 2(b).

The full-energy peak was determined by a single Gaussian fit. The pulse heights at these 11 positions along the crystal were fit to a normalized function [6], [7]

$$\frac{\text{LO}}{\text{LO}_{\text{av}}} = 1 + \delta \left( \frac{x}{x_{\text{mid}}} - 1 \right) \quad (1)$$

where  $\text{LO}_{\text{av}}$  represents the average LO of the sample,  $x$  is the distance from the end coupled to readout device, and  $\delta_{(S \text{ or } T)}$  represents the deviation of the LRU. The schematic of the  $\delta$  is shown in Fig. 3. The measurement errors were estimated by repeatedly measuring the LRU of the long crystal. The  $\delta_S$  and  $\delta_T$  mean the results derived from the seed end and tail end of the crystal coupled with the PMT, respectively.

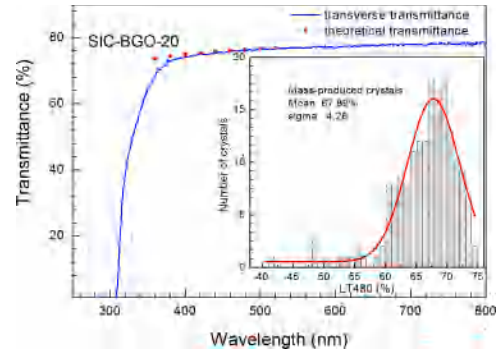


Fig. 4. Optical transmission spectrum of a 600-mm-long BGO crystal along the transversal direction. The theoretical limit of transmittance of BGO is also shown for comparison. Inset: distribution of the optical transmittance at 480 nm along the longitudinal direction of the mass-produced 600-mm-long BGO crystals.

#### IV. OPTICAL QUALITY AND SCINTILLATION PROPERTIES

##### A. Optical Quality and Light Response Uniformity of Mass-Production 600-mm-Long BGO Crystals

Optical quality of the crystals is closely correlated with the LRU. Fig. 4 shows the optical transmission spectrum of one of the mass-produced crystals as a function of wavelength together with the theoretical transmittance limit of BGO. The theoretical transmittance of BGO crystals at certain wavelength is calculated by the following equations [8]:

$$\begin{aligned} T_s &= (1 - R)^2 + (1 - R)R^2(1 - R) + \dots \\ &= (1 - R)/(1 + R) \end{aligned} \quad (2)$$

where

$$R = \left( \frac{n_{\text{BGO}} - n_{\text{air}}}{n_{\text{BGO}} + n_{\text{air}}} \right)^2 \quad (3)$$

where  $n_{\text{BGO}}$  and  $n_{\text{air}}$  are the refractive index of BGO and air, respectively. The difference of the measured transmittance and  $T_s$  may reveal the optical quality of the crystal. The transversal transmittance of the sample is notably in agreement with the theoretical transmittance. The typical longitudinal transmittance (LT) at 480 nm can approach approximately 72%, although slightly worse than the transversal one. To prove the optical quality of the industrial grown BGO crystals, the transmittance of hundreds of 600-mm-long BGO crystals along the longitudinal direction was evaluated. Fig. 4 (inset) shows the distribution of the optical transmittance at 480 nm for nearly 200 crystals. The mean LT is found to be 67.9% with a width of 4.3%. The fraction of crystals with optical transmittance above 60% is about 90%. Fig. 5 shows the distribution of the LRU of the mass-produced 600-mm-long BGO crystals. It is found about 93% of the grown crystals satisfy the requirement of the LRU ( $\delta \leq 20\%$ ).

##### B. Improvement of Optical Quality and Light Response Uniformity

The samples with LRU of  $\delta > 20\%$  and optical transmittance below 58% at 480 nm are unable to satisfy the requirement of the DAMPE detector. We carried out the posttreatments to improve the optical quality and LRU via

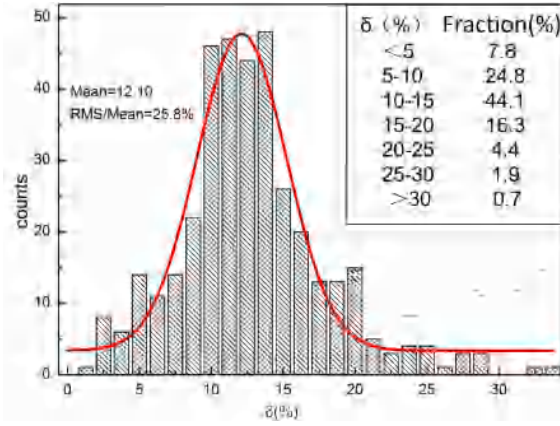


Fig. 5. Distribution of the LRU of the mass-produced 600-mm-long BGO crystals.

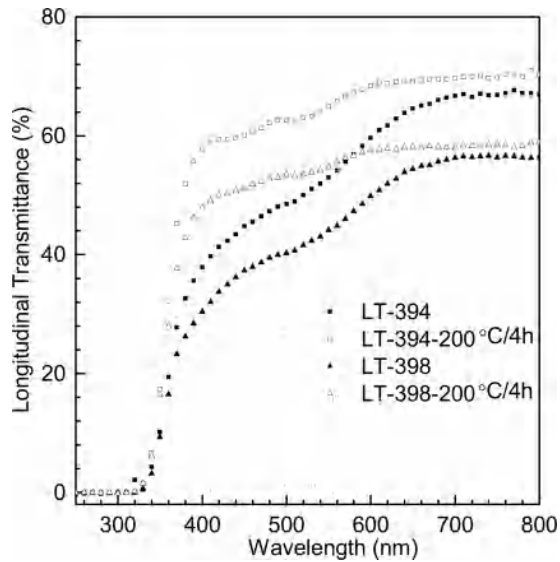


Fig. 6. Optical transmission spectra of the 600-mm-long BGO crystals (SIC-BGO-394 and SIC-BGO-398) along the longitudinal direction before and after air annealing.

TABLE I  
LONGITUDINAL TRANSMITTANCE VALUES BEFORE AND AFTER AIR ANNEALING

Sample number	Transmittance of as-grown crystals (%)	Transmittance of air-annealed crystals (%)	Improvement (%)
SIC-BGO-394	47.29	62.18	14.89
SIC-BGO-398	39.48	52.85	13.37

The longitudinal transmittance values at 480 nm for SIC-BGO-394 and SIC-BGO-398 before and after air-annealing.

air annealing, optimization of reflector materials, and crystal surface treatment.

1) *Effects of Air Annealing*: The samples with transmittance below 58% at 480 nm showed dark red color. The color centers in BGO are commonly related to oxygen vacancies [9], [10]. The oxygen vacancies are the featured point defects in oxide scintillators [11], [12]. Two colored samples named SIC-BGO-394 and SIC-BGO-398 were selected to conduct the air annealing at 200 °C for 4 h. The optical

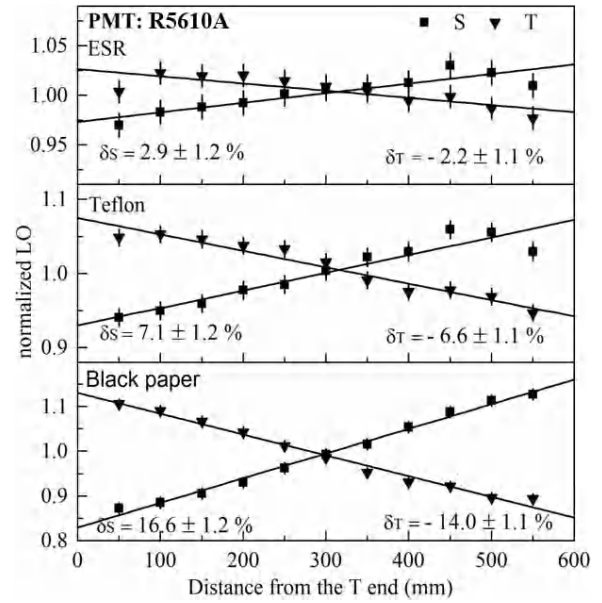


Fig. 7. LRU of the 600-mm-long BGO-SIC-125 crystal wrapped with different reflector materials acquired by Hamamatsu R5610A PMTs. (a) ESR. (b) Teflon. (c) Black paper.

TABLE II  
LRU BEFORE AND AFTER AIR ANNEALING

SIC-BGO-394	$\delta_S/\pm 0.8\%$	$\delta_T/\pm 0.8\%$	Transmittance at 480 nm (%)
As-grown	32.4	-30.6	47.29
Air-annealed	18.2	-16.3	62.18

transmission spectra before and after air annealing are shown in Fig. 6. For the as-grown samples, a clear absorption band with a maximum at 435 nm is observed in both SIC-BGO-394 and SIC-BGO-398 samples, which causes a low transmittance of 40% for SIC-BGO-398 and 47% for SIC-BGO-394 samples. The transmittance is greatly improved up to 52% for SIC-BGO-398 and 62% for SIC-BGO-394 samples after air annealing. It implies that the color centers mainly originate from the oxygen vacancies related defects. The specific values are listed in Table I.

The LRU of the BGO-394 crystal before and after air annealing was evaluated and shown in Table II. The results show that the average light response nonuniformity decreases from 32.4% to 18.2% for  $\delta_S$ , and 30.6% to 16.3% for  $\delta_T$  after air annealing. It is clear that the enhancement of optical transmittance of the crystals positively contributes the LRU. It is worth mentioning that the annealed samples almost satisfy the LRU standard,  $\delta \leq 20\%$ .

2) *Effects of Reflector Materials and Surface Treatment*: According to [13], the higher the reflectivity of the materials used for wrapping crystals, the higher the LO and the energy resolution of the scintillating crystals. Three different reflector materials were tested for the LO uniformity, namely, ESR, Teflon, and black paper. The properties of the reflector materials and the LRU uniformity of BGO-SIC-125 crystal wrapped with these reflector materials are listed in Table III

TABLE III  
 $\delta_S$  AND  $\delta_T$  OF BGO CRYSTALS WRAPPED WITH DIFFERENT REFLECTOR MATERIALS

Reflector materials	Thickness (mm)	Emission-weighted reflection (%)	$\delta_S/\pm 1.2$ (%)	$\delta_T/\pm 1.1$ (%)
ESR	0.06	99.10	2.9	-2.2
Teflon	0.15	92.16	7.1	-6.6
Black paper	0.42	6.29	16.6	-14.0

Properties of reflector materials, and the  $\delta_S$  and  $\delta_T$  of the 600 mm long BGO crystals wrapped with different reflector materials.

TABLE IV  
 LRU OF THE CRYSTAL WITH DIFFERENT SURFACE TREATMENTS

Reflector materials	Six well-polished surfaces		One depolished side surface and five well-polished surfaces	
	$\delta_S/\pm 1.2$ (%)	$\delta_T/\pm 1.1$ (%)	$\delta_S/\pm 1.2$ (%)	$\delta_T/\pm 1.1$ (%)
ESR	2.9	-2.2	36.0	-33.0
Teflon	7.1	-6.6	41.3	-37.2

The LRU of the 600 mm long SIC-BGO-125 crystal with well-polished surfaces and one depolished side surface.

and presented in Fig. 7. It is found that the use of ESR with the highest emission-weighted reflection can achieve the best LRU about  $\delta_S = 2.9\%$  and  $\delta_T = 2.2\%$ , which is much better than the  $\delta_S = 7.1\%$  and  $\delta_T = 6.6\%$  for Teflon and  $\delta_S = 16.6\%$  and  $\delta_T = 14\%$  for black paper. It is clear that high-reflectivity materials can significantly improve the LRU of the crystal. As the increase of reflectivity of the reflector materials, the proportion of photons lost from the crystal decreases. The enhancement of the collection efficiency results in an increase in the average LO of the crystal, which leads to the improvement of the LRU.

It is reported that the crystal surface finish can also alter the light response of the scintillating crystals [14] and affect the light collection efficiency [15]. The LRU can be changed by adjusting the roughness of one or more lateral surfaces of the crystals, such as BGO for L3 [16], lead tungstate for CMS [17], and LYSO for SuperB [18]. Therefore, we have tried to depolish a side surface to study the LRU of the BGO crystal.

We compared the LRU of the same crystal with two different surface treatments, namely, a crystal with six well-polished surfaces and a crystal with five well-polished surfaces and one depolished lateral surface (25 mm  $\times$  600 m) adjacent to the photodetectors. The comparison of the LRU with different surface treatments is listed in Table IV.

When using ESR as the reflector materials, the LRU of the crystal with all well-polished surface is about 2.9%. For the same crystal with one depolished side surface, its LRU significantly deteriorates to about 36%. When using Teflon and black paper as reflector materials, the crystal with one depolished side surface and five well-polished surfaces also shows the worsen LRU compared to the one with all six well-polished surfaces. The harmful effect of surface depolishing could be caused by: 1) the direct light loss at surface and 2) the

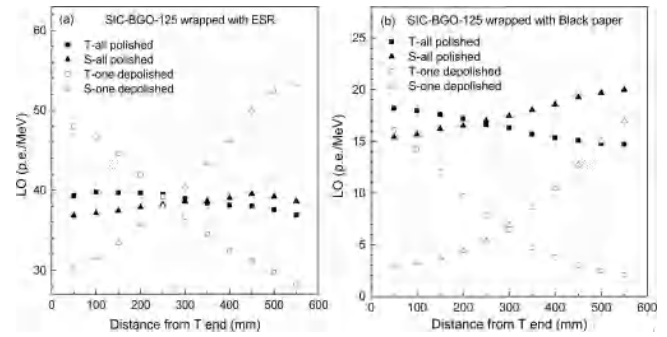


Fig. 8. LRU of the 600-mm-long SIC-BGO-125 crystal wrapped with (a) ESR and (b) black paper.

light path length variation (light collection nonuniformity) [19] due to the change of the surface diffuse reflection on the depolished surface. More quantitatively, we compare the LO at various locations along the longitudinal direction for both surface treatment (Fig. 8). The one surface depolishing treatment significantly increases the LO of the crystal when the radioactive source is near the readout end, but severely reduces the LO of the radioactive source away from the readout end. The significant difference causes the light response nonuniformity. Therefore, a combination of all polished surfaces and ESR as high-reflectivity materials is beneficial to obtain the excellent LRU.

## V. CONCLUSION

Hundreds of 25 mm  $\times$  25 mm  $\times$  600-mm-long BGO scintillating crystals have been produced for DAMPE. It is found that 93% of produced BGO crystals achieve the requirements of LO uniformity of  $\delta \leq 20\%$  and optical transmittance of  $T > 58\%$ . The optical transmittance and the LRU of the colored crystals can be improved by air annealing at 200 °C via the reduction of the oxygen vacancies related absorption bands. The LRU can be improved by the use of ESR reflector materials, but significantly be deteriorated by the side surface depolishing.

## REFERENCES

- [1] *The Nobel Prize in Physics 2013*, Nobelprize.org. Nobel Media AB, 2014.
- [2] J. Chang and J. Wu, "High energy electron and gamma-ray observation by TANSUO mission," in *Proc. 31st ICRC*, Lodz, Poland, Jul. 2009, pp. 1–4.
- [3] J. Chang *et al.*, "The DARK matter particle explorer mission," *Astropart. Phys.*, vol. 95, pp. 6–24, Oct. 2017.
- [4] Z. Ji, H. Ni, L. Yuan, J. Chen, and S. Wang, "Investigation of optical transmittance and light response uniformity of 600-mm-long BGO crystals," *Nucl. Instrum. Methods Phys. Res. A, Accel. Spectrom. Detect. Assoc. Equip.*, vol. 753, pp. 143–148, Jul. 2014.
- [5] Z. M. Ji, H. H. Ni, L. Y. Yuan, J. F. Chen, and S. H. Wang, "Correlation between light response uniformity and longitudinal transmission in 600 mm BGO crystals," *Key Eng. Mater.*, vol. 633, pp. 277–280, Nov. 2015.
- [6] R. Y. Zhu, "On quality requirements to the barium fluoride crystals," *Nucl. Instrum. Methods Phys. Res. A, Accel. Spectrom. Detect. Assoc. Equip.*, vol. 340, pp. 442–457, Mar. 1994.
- [7] J. Chen, L. Zhang, and R.-Y. Zhu, "Quality of a 28 cm long LYSO crystal and progress on optical and scintillation properties," *IEEE Trans. Nucl. Sci.*, vol. 59, no. 5, pp. 2224–2228, Oct. 2012.
- [8] D.-A. Ma and R.-Y. Zhu, "Light attenuation length of barium fluoride crystals," *Nucl. Instrum. Methods Phys. Res. A, Accel. Spectrom. Detect. Assoc. Equip.*, vol. 333, pp. 422–424, Sep. 1993.

- [9] C. L. Melcher, "Thermoluminescence and radiation damage in bismuth germanate," *Nature*, vol. 313, pp. 465–467, Feb. 1985.
- [10] S. G. Raymond, B. J. Luff, P. D. Townsend, X. Feng, and G. Hu, "Thermoluminescence spectra of doped  $\text{Bi}_4\text{Ge}_3\text{O}_{12}$ ," *Radiat. Meas.*, vol. 23, no. 1, pp. 195–202, Jan. 1994.
- [11] F. Meng, Y. Wu, M. Koschan, C. L. Melcher, and P. Cohen, "Effect of annealing atmosphere on the cerium valence state and  $\text{F}^+$  luminescence center in Ca-codoped GGAG:Ce single crystals," *Phys. Status Solidi B*, vol. 252, no. 6, pp. 1394–1401, Jun. 2015.
- [12] C. Wang *et al.*, "Effect of thermal annealing on scintillation properties of  $\text{Ce}:\text{Gd}_2\text{Y}_1\text{Ga}_{2.7}\text{Al}_{2.3}\text{O}_{12}$  under different atmosphere," *Appl. Phys. A, Solids Surf.*, vol. 123, p. 384, May 2017.
- [13] J. Chen, L. Zhang, and R.-Y. Zhu, "Large size LYSO crystals for future high energy physics experiments," *IEEE Trans. Nucl. Sci.*, vol. 52, no. 6, pp. 3133–3140, Dec. 2015.
- [14] J. S. Huber, W. W. Moses, M. S. Andreaco, M. Loope, C. L. Melcher, and R. Nutt, "Geometry and surface treatment dependence of the light collection from LSO crystals," *Nucl. Instrum. Methods Phys. Res. A, Accel. Spectrom. Detect. Assoc. Equip.*, vol. 437, pp. 374–380, Nov. 1999.
- [15] F. Vittori, F. De Notaristefani, T. Malatesta, and D. Puertolas, "A study on light collection of small scintillating crystals," *Nucl. Instrum. Methods Phys. Res. A, Accel. Spectrom. Detect. Assoc. Equip.*, vol. 452, pp. 245–251, Sep. 2000.
- [16] E. Auffray, F. Cavallari, M. Lebeau, P. Lecoq, M. Schneegans, and P. Sempere-Roldan, "Crystal conditioning for high-energy physics detectors," *Nucl. Instrum. Methods Phys. Res. A, Accel. Spectrom. Detect. Assoc. Equip.*, vol. 486, pp. 22–34, Jun. 2002.
- [17] D. Britton, M. Ryan, and X. Qu, "Light collection uniformity of lead tungstate crystals for the CMS electromagnetic calorimeter," *Nucl. Instrum. Methods Phys. Res. A, Accel. Spectrom. Detect. Assoc. Equip.*, vol. 540, pp. 273–284, Dec. 2004.
- [18] L. Zhang, R. Mao, F. Yang, and R.-Y. Zhu, "LSO/LYSO crystals for calorimeters in future HEP experiments," *IEEE Trans. Nucl. Sci.*, vol. 61, no. 1, pp. 483–488, Feb. 2014.
- [19] Y. Wu, A. C. Lindsey, M. Zhuravleva, M. Koschan, and C. L. Melcher, "Growth of inch-sized  $\text{KCa}_{0.8}\text{Sr}_{0.2}\text{I}_3:\text{Eu}^{2+}$  scintillating crystals and high performance for gamma-ray detection," *CrystEngComm*, vol. 18, pp. 7435–7440, Aug. 2016.